Available online at www.sciencedirect.com
SCIENCE DIRECT®
Journal of Chromatography A, 1045 (2004) 161–172
JOURNAL OF CHROMATOGRAPHY A
www.elsevier.com/locate/chroma

Investigation of the surface heterogeneity of solids from reversed-flow inverse gas chromatography

Dimitrios Gavril [a,*], Bernard E. Nieuwenhuys [b]

[a] *Physical Chemistry Laboratory, Department of Chemistry, University of Patras, 26504 Patras, Greece*
[b] *Leiden Institute of Chemistry, Leiden University, P.O. Box 9502, 2300 RA Leiden, The Netherlands*

Received 27 January 2004; received in revised form 8 June 2004; accepted 8 June 2004

Abstract

In the present work, the novel methodology of the inverse gas chromatographic technique of reversed-flow gas chromatography (RF-GC) was applied to the well-studied catalytic oxidation of carbon monoxide over silica supported Pt, Rh and Pt–Rh alloy catalysts. Adsorption energies, local isotherms, local monolayer capacities, surface diffusion coefficients, lateral interaction energies and energy distribution functions are simultaneously determined in a single experiment. The variation of the determined physicochemical parameters against the nature of the studied catalysts (Pt content) is consistent with the observed catalytic activity. The energy distribution functions, estimated by means of RF-GC, give useful information about the "*topography*" and the nature of the active sites on the catalyst surface, similar to those of experimental techniques, such as Thermal Desorption Spectroscopy studies of the adsorption of CO on group VIII noble metal surfaces. The experimentally found results explain the superior activity of $Pt_{0.25} + Rh_{0.75}$ alloy, in comparison to that of the pure Pt and Rh catalysts.

Keywords: Inverse gas chromatography; Reversed-flow gas chromatography; Surface heterogeneity; Catalysts; Adsorption; Site energy distribution; Mathematical modelling

1. Introduction

Adsorption of gases on heterogeneous surfaces has been extensively investigated in the last decades by complimentary studies of theoretical models and experimental systems [1,2]. The nature of the active sites is one of the pervasive problems in heterogeneous catalysis as well as in chromatography. Particularly, in chromatography, the most important property of a site is the average time that the site holds the molecule. In the case of a real solid the information on the heterogeneity of the surface is given by a distribution of the site energies. The formal statement of the adsorption function becomes:

$$\Theta(p, T) = \int_0^\infty \theta(\varepsilon, p, T) f(\varepsilon)\, \mathrm{d}\varepsilon \quad (1)$$

Any two of the functions Θ (experimental adsorption isotherm), θ (unknown local isotherm) and $f(\varepsilon)$ (unknown distribution function of the adsorption energy ε) are needed to calculate the remaining one [1,2]. The methods available for the evaluation of energy distribution functions $f(\varepsilon)$ and consecutively for the surface "*topography*" fall into two main groups: those in which a general analytical form of the distribution function is postulated and the parameters describing it are calculated from the experimental data and those in which no a priori assumption is made about the shape of the distribution.

According to Adamson [3] there is no exact solution to Eq. (1), the reasons being: (a) $\Theta(p, T)$ is an experimental function and will have an experimental error, (b) $\theta(p, T, \varepsilon)$ is taken from some model or other and will not be an exactly correct function because of the limitations of the model, and (c) it is doubtful whether $f(\varepsilon)$, as a one-dimensional distribution function, can fully represent the true picture of surface heterogeneity. It is therefore misleading to talk about a "true" $f(\varepsilon)$. Any pair of $f(\varepsilon)$ and $\theta(p, T, \varepsilon)$ functions that reproduce $\Theta(p, T)$ within the experimental error must be acceptable.

* Corresponding author. Tel.: +30 2610 997144; fax: +30 2610 997144.
E-mail address: d.gavril@upatras.gr (D. Gavril).

0021-9673/$ – see front matter © 2004 Elsevier B.V. All rights reserved.
doi:10.1016/j.chroma.2004.06.015

Inverse gas chromatography has been utilized for the estimation of surface heterogeneity. This is based either on a combination of the net retention volume V_N with the crude CA (condensation approximation) or on a more exact solution by the so-called ACCA (asymptotically correct condensation approximation) method. It is based on replacing the true kernel $\theta(\varepsilon, p, T)$ of the integral Eq. (1), by the combination of a Henry and step isotherm. In terms of V_N, the final solution takes the form:

$$f_{\mathrm{ACCA}}(\varepsilon) = -\left(\frac{j}{N_{\mathrm{m}}}\right)\left(\frac{p}{kT}\right)^2\left(\frac{\partial V_N}{\partial p}\right) \quad (2)$$

where j is the James–Martin compressibility factor and N_{m} the monolayer capacity of the surface. Other improvements of $f_{\mathrm{ACCA}}(\varepsilon)$ are also presented in Ref. [1].

From all the above and other literature data [4,5] one may easily come to the conclusion that the estimation of energy distribution function $f(\varepsilon)$ has been based on the fundamental integral Eq. (1). In the present work a different solution for $f(\varepsilon)$ other than the integral Eq. (1) is used. It uses experimental chromatographic data, obtained by an inverse gas chromatographic method known as reversed-flow gas chromatography (RF-GC), under one single assumption that of a non-linear local isotherm model. Thus, a new gas chromatographic methodology has been developed to measure directly (adsorption, desorption and surface reaction) rate constants, adsorption energies, ε, local adsorption isotherms, $\theta(p, T, \varepsilon)$, adsorption energy distribution functions, $f(\varepsilon)$ [6], surface diffusion coefficients, D_{s} [7], and lateral interaction energies, β [8], on heterogeneous surfaces circumventing altogether the integral Eq. (1).

The most studied reaction in the field of heterogeneous catalysis, oxidation of carbon monoxide was used in order to investigate the nature of the active sites of silica supported Pt, Rh and Pt–Rh alloy catalysts. Carbon monoxide oxidation over Group VIII metals has been extensively studied due to its practical importance for the control of hazard emissions. In addition, selective catalytic oxidation of CO in a hydrogen-rich atmosphere has attracted new interest due to its possible use in fuel cell applications [9]. Most of the catalysts used for the control of automotive emission (three-way catalysts) contain platinum or palladium to catalyze the oxidation of carbon monoxide and hydrocarbons to carbon dioxide as well as rhodium to promote the reduction of nitric oxide to nitrogen [10]. Supported bimetallic catalysts often exhibit certain desirable properties (e.g. improved activity and selectivity, thermal stability, poison resistance, etc.), which are absent in the individual metals. Furthermore, Rh and Pt are by far from the most expensive precious metals. The utilisation of bimetallic catalysts can be advantageous, resulting in a drastic decrease in Pt or Rh usage (e.g. by alloying Pt or Rh with another metal).

2. Experimental

2.1. General

Conventional GC involves the flow of a gaseous mobile phase in a defined direction over a stationary phase or packing that results in the selective retention of solute components. In RF-GC the system is modified; another column (diffusion column) is placed perpendicularly in the center of the chromatographic column (sampling column). The carrier gas flows continuously through the sampling column, while it is stagnant into the diffusion column, as it is shown in Fig. 1. In contrast with conventional GC, where the mobile phase is the center of interest, in RF-GC the solid or liquid substance placed into the diffusion column is under investigation. Thus RF-GC can be assumed as an inverse gas chromatographic method.

Another peculiarity of RF-GC is the sampling procedure of the physicochemical phenomenon, which happens into the diffusion column. Carrier gas flow reversals are done for a short time by using a four-port valve and then the flow is restored in its original direction. The above-mentioned flow reversals procedure results in a short enrichment of the solute quantity into the carrier gas and extra chromatographic peaks are created on the continuous concentration–time curve (chromatogram). The extra peaks are symmetrical and their height or area is proportional to the concentration of the solute in the junction of the diffusion and sampling columns, resulting in a higher sensitivity and accuracy of RF-GC [11].

2.2. Materials

The catalysts studied were pure Pt and Rh, as well as 25% Pt + 75% Rh alloy, all supported on silica gel 60

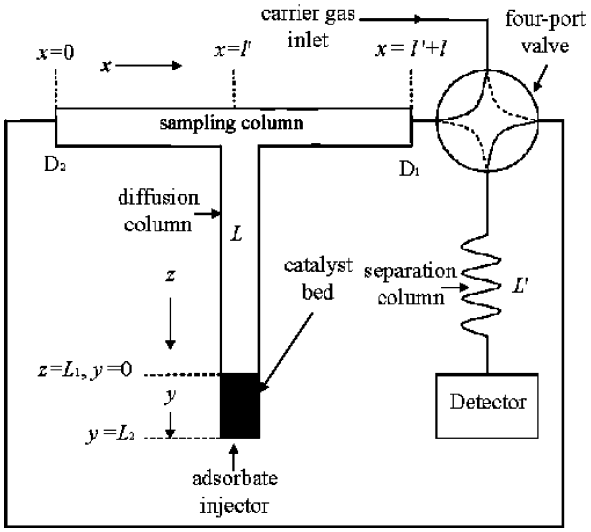

Fig. 1. Experimental setup used for the investigation of the surface heterogeneity of solids, from reversed-flow version of inverse gas chromatography.

(3%, w/w), of Merck (Darmstadt, Germany), $d < 0.063$ mm, 70–230 mesh ASTM. The method of preparation and the surface characterization as well as the activity of the catalysts have been presented previously [12–14].

Hydrogen, from Linde (Patras, Greece) (99.999% pure) was used for the reduction of the catalysts. A mixture of 93% (v/v) helium (99.999% pure) and 7% oxygen (99.999% pure), from B.O.C. Gases (Athens, Greece) was used as carrier gas.

Carbon monoxide from B.O.C. Gases (99.97% pure) was used as reactant, while the product (CO_2) was identified using carbon dioxide from Matheson Gas Products (Athens, Greece) (99.97% pure).

Silica gel (80–100 mesh) from Supelco (Bellfonte, PA, USA) was used as chromatographic material for the separation of carbon monoxide and carbon dioxide.

2.3. Apparatus and procedure

The experimental setup for the application of the RF-GC technique has been presented elsewhere [15–18], and it is also shown in Fig. 1. It comprises: (a) A conventional gas chromatograph equipped with the appropriate detector. The separation column L', filled with the chromatographic material, is also incorporated in the GC oven. (b) The "*sampling cell*", formed by the sampling column $l' + l$ and the diffusion column L, connected perpendicularly to the middle point of the sampling column, is also putted in the chromatographic oven.

Both columns were from stainless steel and free of any material except for a short length (1 cm) at the top of diffusion column L, that contained the catalyst bed and was heated to the same temperature. The stainless-steel separation column L', 45 cm length, filled with silica gel, for the separation of the reactant CO, from its product CO_2, was incorporated in a commercial gas chromatograph, Shimadzu GC-8A, equipped with a thermal conductivity detector for the reactant CO and the product CO_2. The stainless-steel "*sampling cell*" was also incorporated into the gas chromatographic oven. The lengths l' and l of the sampling column were 38 cm each (4 mm i.d.), while the length L of the diffusion column was 117.6 cm (4 mm i.d.). The catalytic bed (0.09–018 g) was put at the top of diffusion column L. Sampling cell ends were connected through a four-port valve, to the carrier gas inlet and the detector, as shown in Fig. 1 of Refs. [15,16].

Before use, the catalysts were reduced at 628 K for 10 h in flowing hydrogen, at a flow rate of 1.0 $cm^3\,s^{-1}$. Then, the whole system was conditioned by heating "in situ" the catalyst bed at 743 K and the chromatographic material at the separation column at 423 K, both for 20 h, under carrier gas flowing. Some preliminary injections of the reactant carbon monoxide were made to stabilize the catalytic behavior. Then, 1.0 cm^3 of CO, under atmospheric pressure was rapidly introduced, with a gas-tight syringe, at the top of the diffusion column L. The reactant oxygen was used in great excess over the other reactant (CO), as a carrier gas mixture component (93%, v/v, He + 7%, v/v, O_2), while carbon monoxide was not retained on the catalytic bed for a long time, but it was eluted with the produced carbon dioxide. After 5 min, a continuous concentration–time curve for to both reactant (CO) and product (CO_2) was established and recorded. During this period flow reversals of carrier gas direction, for 5 s, were made and then the gas was again turned to its original direction, simply by switching the four-port valve from one position to the other and vice-versa. This time period was shorter than the gas hold-up time in column sections l', l and L'. When the gas flow was restored to its original direction, two sample peaks were recorded, such as those shown in Fig. 2 of Ref. [17].

The first peak belongs to the reactant CO and the second to the product CO_2. Repeating the above reversal procedure for many times at each temperature, two series of sample peaks were recorded; each pair of them corresponds to a different time from reactant injection. The working temperature range was 553–748 K, for the catalyst while, for the chromatographic material it was kept constant at 358 K. The variation in the temperature along the catalytic bed was measured by a digital thermometer (Fluke 2190A) and was smaller than 1 K. The volumetric carrier gas flow rate, at ambient temperature was 1.0 $cm^3\,s^{-1}$. The pressure drop along the whole system was 0.33 atm.

3. Theoretical

3.1. Mathematical model

The sampling peaks are predicted theoretically by the "chromatographic sampling equation", describing the concentration–time curve of the sampling peaks created by the flow reversals. The area or the height H, of the sampling peaks is proportional to the concentration of the substance under study, at the junction, $x = l'$, of the sampling cell, at time, t, from the beginning of the experiment [11]. If $\ln H$ is plotted against time, t, for each substance, a so called "*diffusion band*", is obtained. An example is shown in Fig. 3 of Ref. [18].

The calculations based on the following mathematical model: (a) two mass balance equations for the gaseous concentrations c_y (mol cm^{-3}) and c_z (mol cm^{-3}) of CO in the regions y and z of the diffusion column, respectively; (b) the rate of change of the adsorbed concentration c_s (mol g^{-1}); and (c) the isotherm for the local adsorbed equilibrium concentration c_s^* (mol g^{-1}) of CO on the solid, at time t. The term "local" for c_s^* means with respect to time t, i.e. involving not all adsorption energy sites, but only those active at time t. The expression "equilibrium concentration" for c_s^* means microscopically reversible, not a statical one. The solution of this mathematical model under given initial conditions leads to the following relation for the peak height H.

$$H^{1/M} = \sum_{i=1}^{4} A_i \exp(B_i t) \tag{3}$$

where H is the height of the experimentally obtained chromatographic peaks, M the response factor of the detector and t the time. The gaseous concentration c_y above the solid at $y = 0$ of the solid bed and the local adsorbed equilibrium concentration, c_s^*, of the absorbate as a function of time, t, are given as follows [7]:

$$c_y = \frac{vL_1}{gD_1} \sum_{i=1}^{4} A_i \exp(B_i t) \tag{4}$$

$$c_s^* = \frac{a_y}{a_s} k_1 \frac{vL_1}{gD_1} \sum_{i=1}^{4} \frac{A_i}{B_i} [\exp(B_i t) - 1] \tag{5}$$

where D_1 is the diffusion coefficient of CO into the carrier gas, v the corrected linear flow velocity of the carrier gas, L_1 the length z of the diffusion column, a_y the cross-sectional area of the void space in the solid bed, a_s the amount of solid per unit length of bed ($g\,cm^{-1}$) and k_1 (s^{-1}) the adsorption rate constant of CO on the surface. All above quantities (except M, v, L_1, a_y, a_s) contained in the above equations, including the pre-exponential functions, A_i, the coefficients of time, B_i, the effective diffusion coefficient of CO in the solid bed D_y, the desorption k_{-1} (s^{-1}) and surface reaction k_2 (s^{-1}) rate constants are calculated by non-linear regression analysis with a GW-BASIC PC programme [7] from the experimental pairs H, t.

A non-linear local isotherm model, going to the Langmuir isotherm in middle pressures and to a linear form at low pressures, was selected:

$$\theta(p, T, \varepsilon) = 1 - \exp(-Kp) \tag{6}$$

where K is the local Langmuir's constant.

The final equations giving local isotherms, $\theta(p, T, \varepsilon)$, adsorption energies, ε, local monolayer capacities, c_{max}^* [19], energy distribution functions for adsorption, $\varphi(\varepsilon; t)$ [6], surface diffusion coefficient D_s [7], and lateral interaction energy β [8], are:

$$\varepsilon = RT[\ln(KRT) - \ln(RT) - \ln K^0] \tag{7}$$

$$c_{max}^* = c_s^* + \frac{\partial c_s^* / \partial c_y}{KRT} \tag{8}$$

$$\theta = 1 - \frac{1}{c_{max}^*} \frac{\partial c_s^* / \partial c_y}{KRT} \tag{9}$$

$$f(\varepsilon) = \frac{1}{RT} \left[\frac{KRT(\partial c_s^* / \partial t)}{\partial (KRT)/\partial t} + \frac{\partial^2 c_s^* / \partial c_y \partial t}{\partial (KRT)/\partial t} - \frac{\partial^2 c_s^* / \partial c_y}{KRT} \right] \tag{10}$$

$$\varphi(\varepsilon; t) = \frac{\theta f(\varepsilon)}{c_{max}^*} \tag{11}$$

$$D_s = \frac{D_1 \varepsilon_M^2 - D_y}{K^0(1-\theta)} \exp\left(-\frac{\varepsilon}{RT}\right) \tag{12}$$

$$\beta = \frac{1}{c_y} \left[\frac{\exp(KRTc_y) - 1}{KRT} - \frac{c_s^*}{C_2} \right] \tag{13}$$

where ε_M is the macro void fraction in the bed. KRT as function of time from the experimental sample peaks H, t has been described in detail elsewhere [6–8]. The result is:

$$KRT = \frac{gD_1}{vL_1} \left\{ \frac{\sum_i A_i B_i^2 \exp(B_i t)}{[\sum_i A_i B_i \exp(B_i t)]^2} - \frac{1}{\sum_i A_i \exp(B_i t)} \right\} \tag{14}$$

Other unknowns on the right-hand side of Eqs. (8)-(10) and (13) are the derivatives $\partial c_s^* / \partial c_y$, $\partial c_s^* / \partial t$ and $\partial^2 c_s^* / \partial c_y \partial t$, being functions of the coefficients of time, B_i, and pro-exponential coefficients, A_i, of Eq. (3), of the rate constants (k_1, k_{-1} and k_2), of the corrected linear flow velocity of the carrier gas, v, of the diffusion coefficient of CO into the carrier gas, and of geometrical characteristics of the diffusion column, L (a_y, a_s, L_1) [6–8].

The majority of IGC measurements require infinite dilution and fast equilibration of the injected solute between the stationary and mobile phase. These demands are also achieved by using reversed-flow IGC methodology. However, the usual inverse gas chromatography, in which the stationary phase is the main object of investigation, is a classical elution method that it neglects the mass transfer phenomena and it does not take into account the sorption effect. In contrast to that integration method, the novel methodology of reversed-flow gas chromatography (RF-GC), although being an inverse gas chromatographic technique, it is a differential method not depending either on retention times and net retention volumes, V_N, or on broadening factors and statistical moments of the elution bands. The results of the new methodology of RF-GC are based on a non-linear adsorption isotherm model and rate measurements over an extended period of time. Thus, RF-GC is a time-resolved chromatography, exhibiting different behavior with sampling time [6,7].

3.2. Calculations

The narrow fairly symmetrical "*sample peaks*" created by the flow reversals were recorded and their heights, H, were measured, together with the corresponding time t. These pairs H, t of experimental values are the variables of Eq. (3). By introducing them into the data lines of the GWBASIC program given in the Supporting Information of Ref. [7], together with other quantities required by the input lines 190–350, the physicochemical parameters and functions defined by Eqs. (4), (5) and (7)-(13) are calculated.

The dead volume of the system (columns, valve, detector, etc.) does not affect the results of RF-GC. The geometric characteristics of sections L_1 and L_2 (empty volumes and lengths) of the diffusion column are only necessary for the

estimations, which can easily and accurately be measured, e.g. by measuring the mass of the respective section of the diffusion column, having filled it by water at a fixed temperature. The quantities ε, c^*_{max}, θ, c^*_s, $\phi(\varepsilon; t)$, D_s and β are estimated and saved in a simple data file. Importing these data in usual PC software like Origin, curves of pairs of the above mentioned quantities are constructed (e.g. θ against ε, $\phi(\varepsilon)$ against ε, etc.).

4. Results and discussion

The adsorption of diatomic molecules, such as CO, on a metal surface can be considered as competition between molecular and dissociative adsorption [10]:

$$CO_{(g)} \leftrightarrow CO_{(ads)} \rightarrow C_{(ads)} + O_{(ads)} \quad (15)$$

Molecular adsorption of CO is relatively strong on many noble metal surfaces. Consequently, CO may undergo both dissociative and molecular adsorption on the same surface depending on experimental conditions. It is often observed that molecular adsorption prevails at lower temperatures and dissociative adsorption occurs at higher temperatures. This pattern may be caused by kinetics; the activation energy for dissociative adsorption is too high at lower temperatures. There may be a thermodynamic reason; if the number of surface sites at which adsorption can take place is equal for molecular and dissociative adsorption, the surface can accommodate twice as many molecules in the molecular as in the dissociated state. Hence, molecular adsorption will prevail if the heat of dissociative adsorption is not much greater than the heat of molecular adsorption. The entropy change for adsorption is negative and, consequently, at sufficiently higher temperatures desorption will occur. In the case considered previously, only half the number of molecules can be adsorbed in the dissociative state in comparison with those in the molecular one. As a result, the entropy of the system will be lower for molecular adsorption and dissociation can occur at higher temperatures.

Carbon monoxide dissociative adsorption [20], carbon monoxide, oxygen and carbon dioxide adsorption [16], carbon monoxide oxidation [15] over various silica supported Pt, Rh, and Pt–Rh alloys catalysts have been studied by utilizing RF-GC methodologies. As result, kinetic parameters as rate constants, activation energies, fractional conversions [17,18], surface diffusion coefficients have been determined. The main conclusions of these studies are: (a) There is a characteristic temperature of maximum catalytic activity, T_{max}, for every catalyst. The temperatures found by RF-GC are equal to those found by other workers, for the same catalysts, using other techniques [12–14]. (b) The experimental data for carbon monoxide adsorption over the studied catalysts (in the absence of oxygen in the carrier gas), at temperatures higher than 300 °C, suggest that the adsorption of CO is a dissociative process, following the Boudouard reaction [16,18,20].

$$2CO_{(g)} \rightarrow C_{(ads)} + CO_{2(g)} \quad (16)$$

(c) The bimetallic catalysts exhibit higher catalytic activity at lower temperatures in comparison to pure Pt and Rh ones. Other workers have also observed this synergism for Pt–Rh bimetallic catalysts [12–14]. (d) It has been observed that the diffusion of CO into the catalyst pores is the rate determining step at temperatures below the temperature of maximum catalytic activity, T_{max} [17,18].

In addition, there is a lot of information concerning the nature and the different groups of the active sites concerning carbon monoxide oxidation over Group VIII metals. For these reasons we selected to present the various adsorption parameters related with the oxidation of carbon monoxide over the silica supported platinum, rhodium and $Pt_{0.25}$–$Rh_{0.75}$ alloy catalysts, in the temperatures of maximum catalytic activity.

The physicochemical parameters determined by RF-GC, related with the investigation of the surface heterogeneity are the local energy of adsorption, ε, the local isotherm, θ, the local maximum monolayer capacity, c^*_{max}, the local adsorbed equilibrium concentration of CO, c^*_s, the energy distribution function, $\varphi(\varepsilon; t)$, as well as the surface diffusion coefficient, D_s and the lateral interaction energy, β.

The variation of the local isotherm θ against the local adsorption energy ε is shown in Fig. 2.

These plots can be compared with the plots constructed by the method of Adamson and Ling as shown in Ref. ([1], p. 430). The shapes of the curves of Fig. 2 resemble those given by Adamson and Ling at temperatures above the critical temperature. Our experiments were carried out in a temperature range (280–450 °C) much higher than the critical temperature of CO (−140 °C). All isotherms of Fig. 2 have an inflection point around $\theta = 0.5$, which corre-

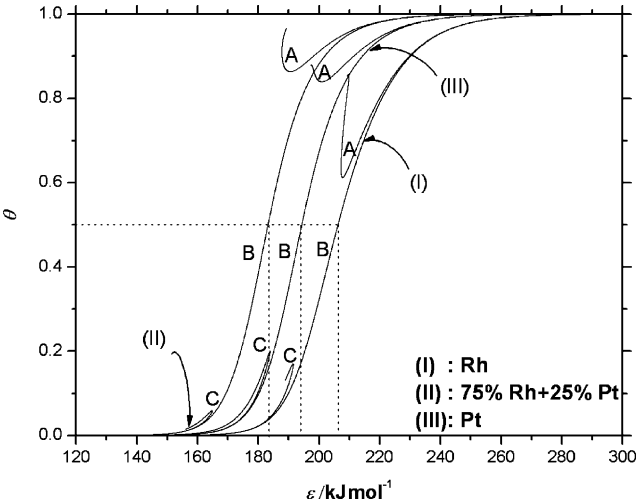

Fig. 2. Plots of local isotherms θ vs. the local adsorption energy ε for the adsorption of carbon monoxide on: (I) pure Rh, at 445 °C, (II) bimetallic $Pt_{0.25}$–$Rh_{0.75}$, at 390 °C, and (III) pure Pt catalysts, at 425 °C. Groups A, B and C indicate the three different kinds of active sites corresponding to different surface coverage.

sponds to different adsorption energies for the three studied catalysts in the different T_{max} temperatures. Parts A and C do not deviate energetically much from the main curve B, but as it will be shown these parts reveal interesting information about the "*topography*" of the active sites on the heterogeneous surface. Similar curves have also been calculated theoretically through Monte Carlo simulations for adsorption on randomly heterogeneous surfaces. The different parts of their plots have been attributed to areas of the surface characterized by different degrees of heterogeneity [21].

The found local adsorption energies, ε, denoted as well as $-\Delta U^0$, are defined as the difference between the energy of the minima known as adsorption sites and the average energy of the molecules in the equilibrium bulk state. Their values are relatively high, covering a range from 140 to 280 kJ mol^{-1} (33–67 kcal mol^{-1}). Such values indicate a strong interaction between CO and the catalyst surface and they are typically of the studied catalysts and the high temperatures (390, 425 and 445 °C, much above the critical temperature of carbon monoxide) at which the kinetic tests were carried out. Bearing in mind, the high values of the found adsorption energies and the experimental conditions ($T > 390$ °C and $P = 1.33$ atm), the found adsorption energies are reasonable for the cleavage of C–O bond of the adsorbed state of CO [10]. The experimentally measured temperatures may reflect more that of the gas phase than of the solid bulk phase. Consequently, it is doubtful that the surface is truly isothermal under high CO conversions. However, qualitative information concerning the various groups of active sites can be derived.

Coming back to the isotherms of Fig. 2, one can also note: (i) First, carbon monoxide molecules are initially absorbed on high adsorption energy sites in the minimum of potential energy of the surface (part A of the isotherm) and, finally, on sites of lower adsorption energy (part C). Part B of the isotherm covers the whole spectrum of local adsorption energies, ε and surface coverage, θ. (ii) Second, the same value of surface coverage, θ, e.g. the inflection point at $\theta = 0.5$ is observed for different values of adsorption energy for the three studied catalysts. The values of adsorption energies ε, at $\theta = 0.5$ are summarized in Table 1. It is obvious that the same surface coverage is achieved at sites of lower adsorption energy for the most active bimetallic catalyst, according to the observed catalytic activity and the known synergism between Pt and Rh [12–14].

Table 1
Adsorption energies ε (kJ mol^{-1}) at the inflection point ($\theta = 0.5$), in the temperatures of maximum catalytic activity, for the adsorption of CO over the studied silica supported Pt–Rh bimetallic and pure Pt and Rh catalysts

Catalyst	T (°C)	ε (kJ mol^{-1})
Rh	445	206
$Pt_{0.25}$–$Rh_{0.75}$	390	183
Pt	425	195

Another surface parameter estimated by the presented methodology, giving a quantitative description of carbon monoxide adsorption on the different studied heterogeneous surfaces is the local maximum monolayer capacity, c^*_{max}. Bearing in mind that a heterogeneous surface includes active centers of different adsorption energy (cf. Fig. 2), different values of c^*_{max} corresponding to the active sites of different ε are reasonable. Semi logarithmic plots of the local maximum monolayer capacities, c^*_{max}, against the corresponding energies of adsorption, ε, for the adsorption of CO on the studied catalysts, are given in Fig. 3.

The following conclusions can be drawn from the curves of Fig. 3, describing the variation of c^*_{max} values against ε: (i) They consist of two linear parts; The second part, which corresponds to an almost constant value of c^*_{max}, in high values of adsorption energy (adsorption on the minima of potential energy of the surface) and the first part, corresponding to smaller values of ε, in which the c^*_{max} values seem to increase with decreasing ε. However, the latter does not mean that the active sites of smaller adsorption energy can adsorb such large amounts of CO. These rather high values of maximum local concentration are apparent ones corresponding to a theoretical monolayer of CO adsorbed molecules. The product of the local isotherm θ and the maximum monolayer capacity c^*_{max} gives the true quantity of adsorbed CO. (ii) From the second linear part of Fig. 3 curves, corresponding to CO strong chemisorption on the minima of potential energy of the surface, the maximum monolayer adsorbed concentration of carbon monoxide can be estimated. These values are referred in Table 2, and they are different for every catalyst. c^*_{max} values increase with the content of Pt in the catalyst. This is consistent with the general observation that CO is mainly adsorbed on Pt sites and oxygen on Rh

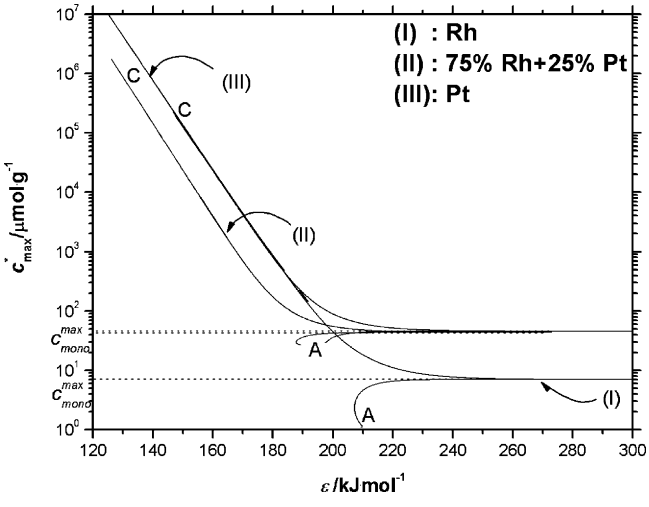

Fig. 3. Semi logarithmic plots of maximum local monolayer capacities c^*_{max} against the corresponding energies of adsorption, ε, at the temperatures of maximum catalytic activity, for carbon monoxide's adsorption over silica supported: (I) rhodium, (II) $Pt_{0.25}$–$Rh_{0.75}$ alloy, and (III) platinum catalysts. Symbols A, B and C indicate the three different groups of active sites corresponding to different monolayer capacities.

Table 2
Maximum local monolayer adsorbed concentrations of carbon monoxide on the minima of potential energy of the surface, c_{max}^{mono} (μmol g^{-1}), for the pure Pt, Rh and the Pt–Rh alloy catalysts, at the temperature of maximum catalytic activity

Catalyst	T (°C)	c_{max}^{mono} (μmol g^{-1})
Rh	445	7.00
$Pt_{0.25}$–$Rh_{0.75}$	390	42.89
Pt	425	46.03

sites [12–14]. (iii) Only parts A (corresponding to the initial gaseous concentration c_y of the ascending branch of c_y versus, t) are shown in the plots of Fig. 3, while C ones (corresponding to the final gaseous concentration, c_y, of the descending branch of $\ln H$ versus t) are identified with the rest of the plot.

The question naturally arising is how the energy distribution function, $\varphi(\varepsilon; t)$ is distributed over the ε values. This distribution is usually described as the "*topography*" of the surface. Such distributions for the adsorption of carbon monoxide over the three studied catalysts are shown in Fig. 4. In all cases, the curves have a purely Gaussian shape. This finding is an experimental fact and not an assumption for the distribution function, as made several times in the past, e.g. by Steele [22] and Jagiello [23]. However, it should be noted that a proper comparison between the distribution functions obtained by RF-GC, for the interaction of CO with Pt–Rh alloy catalysts, which are described here, and those determined through the integral Eq. (1), for different adsorbate-adsorbent systems, at different experimental conditions is not possible.

The plots of $\varphi(\varepsilon; t)$ against ε, can also be normalized to unity with respect to the energy of adsorption. The total area under the curve must be:

$$\int_{\varepsilon_1}^{\varepsilon_2} \varphi(\varepsilon)\, \mathrm{d}\varepsilon = 1 \qquad (17)$$

This is easily achieved by calculating the areas under the curves of Fig. 4 between the extreme values ε_1 and ε_2 of the experimentally found ε. Division of the integral in the left side of the previous equation by a normalizing factor like the zeroth moment of the distribution with respect to ε, satisfies equality to one [24].

The different curves of Fig. 4 obtained for the adsorption of CO over the studied catalysts indicate the existence of three groups of active sites with respect to adsorption energy ε. From this point the revelation of the physical meaning of parts A and C begins.

Generally, the first kind of active sites (A), which correspond to higher values of ε, form a narrower distribution in comparison with the main curve B, while the third kind of active sites (C), corresponding to lower energies of adsorption form a very narrow abnormal distribution. More quantitative information for the relative populations of the different kinds of active sites with respect to energy can be obtained from the areas below the curves of $\varphi(\varepsilon; t)$

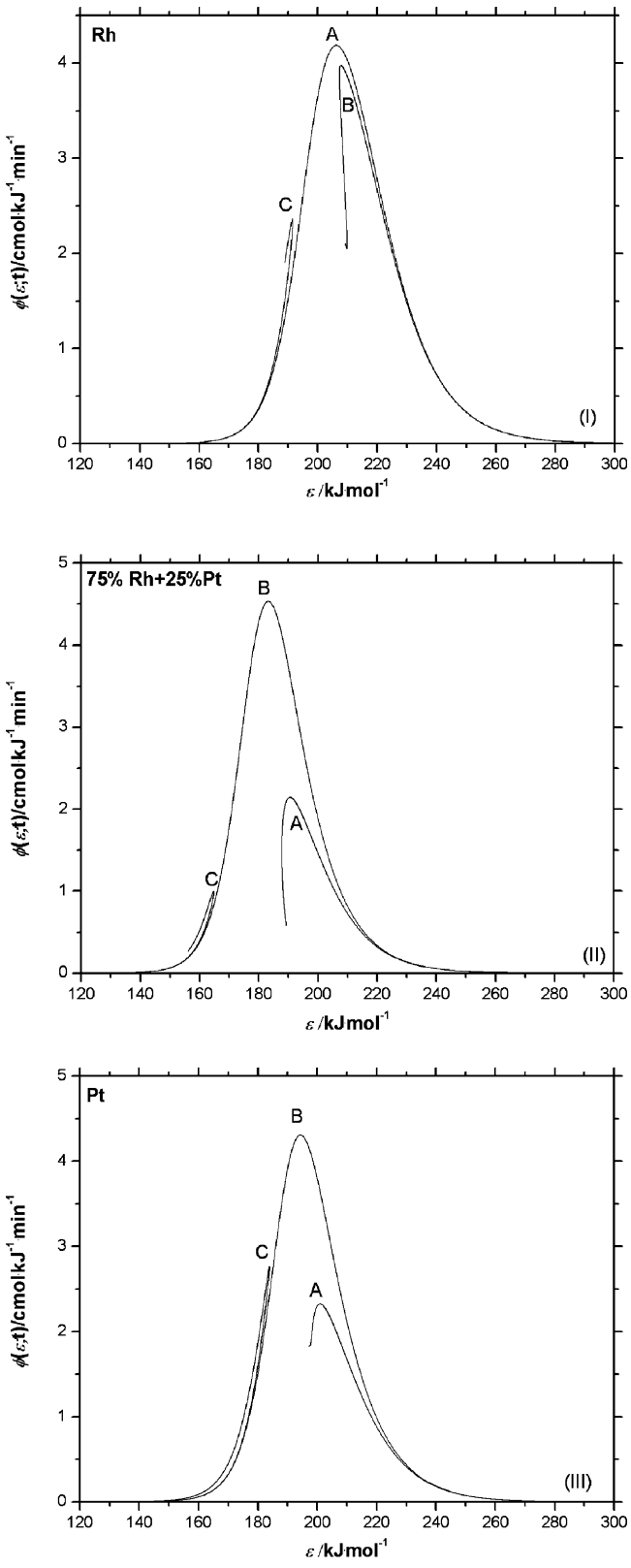

Fig. 4. Variation of the energy distribution function $\varphi(\varepsilon; t)$ vs. the local adsorption energy, ε, at the temperatures of maximum catalytic activity, for the adsorption of carbon monoxide on: (I) Rh_{pure}, (II) bimetallic $Pt_{0.25}$–$Rh_{0.75}$, and (III) Pt_{pure}, silica supported catalysts. Groups A, B and C indicate the three different kinds of active sites corresponding to higher, intermediate and lower energies of adsorption, respectively.

Table 3
Percentages of the areas under the curves of the energy distribution function $\varphi(\varepsilon; t)$ against the structural parameter, t, time from the beginning of the experiment, corresponding to the different kinds of active sites (A, B and C), at the temperatures of maximum activity, for CO oxidation, over the studied catalysts

Catalyst	T (°C)	A (%)	B (%)	C (%)
Rh	445	20.5	30.7	48.8
$Pt_{0.25}$–$Rh_{0.75}$	390	9.5	37.3	53.2
Pt	425	12.0	32.4	55.5

against the structural parameter time, t (recall that RF-GC is a time-resolved chromatography, exhibiting different behavior with sampling time). Such a calculation is presented in Table 3. An interesting observation is the variation of the percentage of the most active sites A. The percentage of the most active sites A, for CO adsorption increases with the content of Pt in the catalyst. This is consistent with the general observation that CO is mainly adsorbed on Pt. Furthermore, in unpublished results concerning the adsorption of carbon monoxide on the studied surfaces (in the absence of oxygen in the carrier gas) the respective percentages of active sites A have much higher values (approximately, twice compared to those of CO oxidation). The explanation of the small values of the percentage of active sites A, for the oxidation reaction in comparison with the respective values for the adsorption of CO, can be attributed to the effect of chemisorbed oxygen on the minima of potential energy (recall that the surface is pre-exposed to oxygen, which is a constitute of the carrier gas, that it is dissociatively adsorbed), as well as to a possible deactivation of these sites (e.g. carbon deposition due to CO dissociative adsorption).

More information about the different groups of active sites of Fig. 4, can been extracted, from the plots of the local isotherm θ and the distribution function $\varphi(\varepsilon; t)$, against the local adsorbed equilibrium concentration of CO, c_s^*, in a semi-logarithmic scale, over the studied Pt, Rh and Pt–Rh alloy catalysts, shown in Figs. 5 and 6. It should be noted that the term local means with respect to time. Thus, local adsorption isotherms are referred to the coverage of the various groups of active sites corresponding to a particular adsorption energy varying with time. Local adsorption isotherms have been presented [5,6,19].

From the variation of the local isotherm, θ, against, c_s^* it is clear that the group A active sites describe the chemisorption of CO, at high coverage values until the formation of the monolayer. Then, larger amounts of CO are adsorbed, less strongly, on sites of lower energy (groups B and C). This behavior, in which lower amounts of CO are strongly adsorbed on active sites of group A, is consistent with the specific nature of chemisorption.

By plotting the distribution function, $\varphi(\varepsilon; t)$, against the local adsorbed concentration of CO, c_s^* the different kinds of active sites groups shown in Fig. 6, are clearly resolved. It can be considered, for reasons of comparison that lower c_s^* values correspond to higher ε values and vice-versa. The

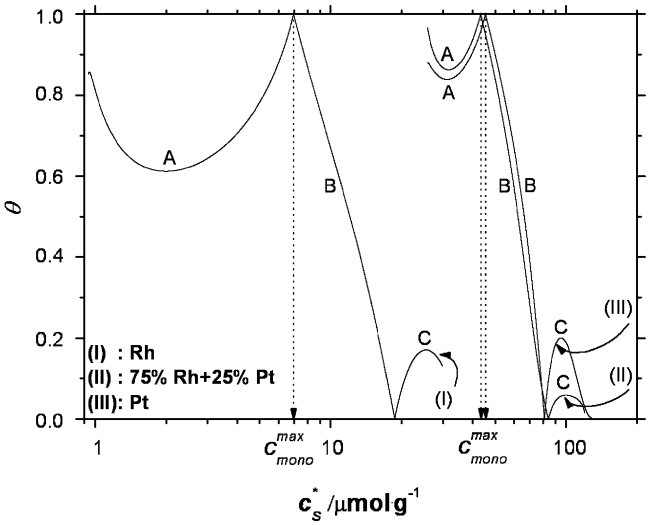

Fig. 5. Semi logarithmic plots of the local isotherms, θ, against the local equilibrium adsorbed concentration, c_s^*, at the temperatures of maximum catalytic activity, for carbon monoxide's adsorption over silica supported: (I) rhodium, (II) $Pt_{0.25}$–$Rh_{0.75}$ bimetallic, and (III) platinum catalysts. A, B and C symbolize the three different groups of active sites corresponding to different concentrations of adsorbed CO.

reason is that the two limiting curves: curve (III), corresponding to Pt–Rh bimetallic catalyst, describes a kinetic experiment at 390 °C and curve (I), corresponding to pure Rh one, describes an experiment at 445 °C. It is obvious that with increasing temperature and, consequently, adsorption energy, the probability of CO adsorption on active sites of group A increases, as is expected for a specific process such as chemisorption. It should be noted that this is true for the forward step of CO chemisorption. For the net adsorption result (considering desorption as well) the opposite is true.

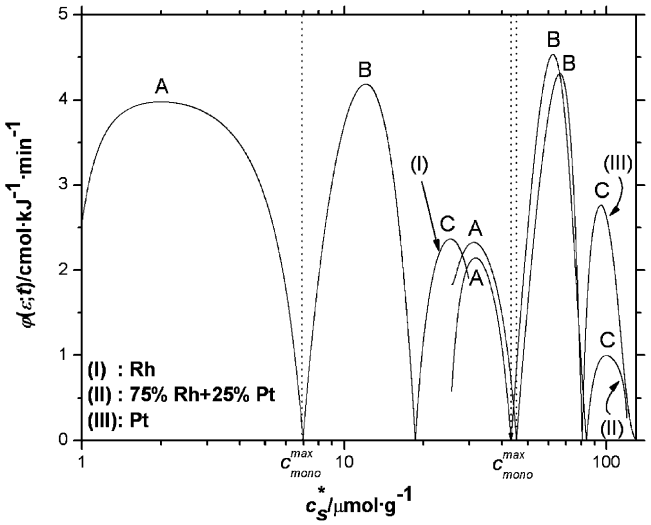

Fig. 6. Semi logarithmic plots of the energy distribution function, $\varphi(\varepsilon; t)$, vs. the local equilibrium adsorbed concentration, c_s^*, of CO on: (I) pure Rh, at 445 °C, (II) $Pt_{0.25}$–$Rh_{0.75}$ alloy, at 390 °C, and (III) pure Pt catalysts, at 425 °C. Groups A, B and C indicate the three different kinds of active sites shown in the plots of the energy distribution function vs. the energy of adsorption.

Furthermore, the largest amount of CO is adsorbed on the most active Pt–Rh bimetallic catalyst at a much lower value of temperature and adsorption energy. On the other side, the probabilities of active sites of groups B and C increase with decreasing temperature and adsorption energy.

Another subject of great interest in adsorption studies is that of the motion of the adsorbed molecules on a heterogeneous surface. Surface diffusion provides a competitive mechanism for the mass transport from or to the pores of a solid. Generally, the diffusion coefficient values increase approximately with the square of the mean free path. Bearing in mind that the mean free path has a magnitude of 100 molecular diameters in the gas phase and 1 molecular diameter in the solid phase, a difference in magnitude of $100^2 = 10^4$ is reasonable.

The diffusion coefficients calculated by means of Eq. (12) increase with increasing temperature and follow an Arrhenius-type temperature dependence. The magnitude of D_s values of the present work is comparable with those obtained by other experimental techniques such as the chromatographic method, the frequency response method and the differential adsorption bed method [25–27] as well as Monte Carlo simulations [28]. Semi-logarithmic plots of the energy distribution function, $\varphi(\varepsilon; t)$, versus the experimentally measured D_s values of CO on the various active sites of the studied catalysts are given in Fig. 7.

The following conclusions can be drawn from these curves: (i) They have a Gaussian shape. (ii) The D_s values obtained by RF-GC for the adsorption of CO on the studied catalysts range from 10^{-6} to $10\,cm^2\,s^{-1}$. Bearing in mind that the values of the diffusion coefficient of CO in He, calculated by the Fuller–Schetler–Giddings equation [29], range from 2.09 (at 390 °C) to $2.40\,cm^2\,s^{-1}$ at (445 °C), the experimentally found D_s values are reasonable under the experimental conditions of temperature and pressure ($T = 390$–445 °C and $P = 1.33$ atm). (iii) They indicate the existence of three kinds of active sites. A basic difference between the distributions of active sites A and C is that they correspond to lower and higher values of D_s respectively. (iv) The D_s values calculated by means of Eq. (12) cover a wide range of values and show that strong chemisorption as well as less strong adsorption of CO molecules occur. In the early stage of adsorption, the adsorbate mainly occupies active sites probably in larger pores of higher mobility until the formation of a monolayer, which occurs in smaller pores where the mobility of CO is the lowest (A sites). Then the adsorbate progressively occupies larger pores in larger distance from the surface resulting in higher observed surface diffusivity due to the lower affinity of these pores towards the adsorbate (B and C active sites). It should be noted that at the studied temperatures of maximum catalytic activity the reaction of carbon monoxide oxidation is kinetically and non diffusion controlled [18].

It is obvious that the studied silica supported Pt–Rh alloys are characterized by heterogeneity. A general cause of surface heterogeneity is that of absorbate-absorbate interaction

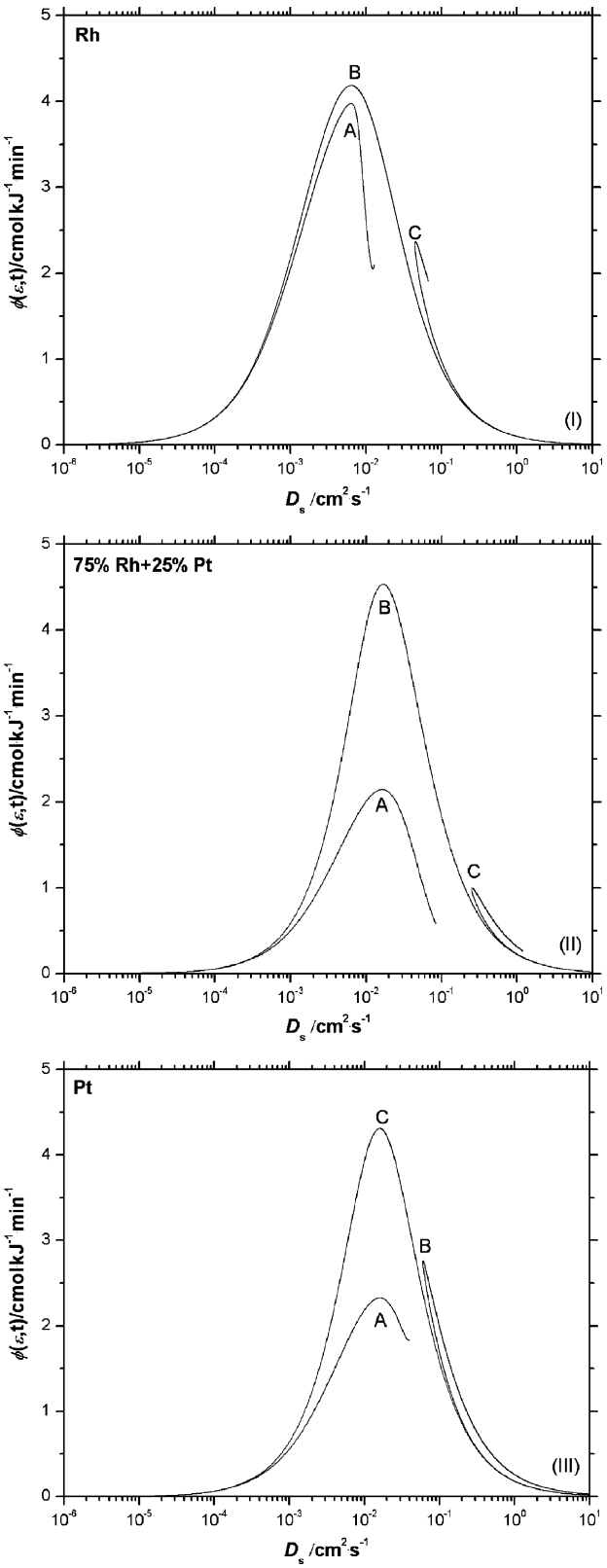

Fig. 7. Semi logarithmic plots of the energy distribution function $\varphi(\varepsilon; t)$ vs. the surface diffusion coefficient, D_s, at the temperatures of maximum catalytic activity, for carbon monoxide's adsorption over silica supported: (I) rhodium, (II) $Pt_{0.25}$–$Rh_{0.75}$ bimetallic, and (III) platinum, silica supported catalysts. Groups A, B and C symbolize the three different kinds of active sites corresponding to different degrees of CO molecules mobility.

which is associated with *island* formation. Extensive experimental studies of CO oxidation on transition-metal surfaces and simple kinetic model calculations [30] indicate that the reaction $O + CO \rightarrow CO_2$ occurs at the boundary between domains of adsorbed atomic oxygen and adsorbed CO, respectively.

Such kind of information is also possible by the methodology presented; the energy distribution function, $\varphi(\varepsilon; t)$, was plotted against the calculated product of the lateral interaction energy and local surface coverage, $\beta\theta$, as shown in Fig. 8. From the curves of Fig. 8, the following observations can be made.

First, the existence of three kinds of adsorption active sites with respect to $\beta\theta$. Second, active centers A and C form distributions at negative and positive values of $\beta\theta$, respectively, while active sites B form narrower distributions at values of $\beta\theta$ near to zero. The physical meaning of negative $\beta\theta$ values is that they indicate repulsive surface interactions, while positive $\beta\theta$ values are indicative of lateral attractions [31]. Lateral *attractions*, ascribable to van der Waals forces, are relatively weak in comparison to chemisorption energies, and it appears that in chemisorption, *repulsion* effects may be more important. These can be of two kinds: A *short-range repulsion* between the electron clouds of adjacent CO adsorbed molecules or a *long-range repulsion* due to a dipole field (if adsorption bond formation polarizes the absorbate, or strongly orients an existing dipole, the absorbate film will consist of similarly aligned dipoles). As discussed by Fowler and Guggenheim [31] neighboring sites will be occupied more often than the statistical expectation if the situation is energetically favored (β positive $\rightarrow$ "*patchwise*" topography). Conversely, if there is lateral repulsion (β negative), nearest neighbor sites will be less frequently occupied than otherwise expected ("*random*" topography). Consequently, adsorption of CO molecules on the minima of potential energy (A sites) is accompanied with repulsive forces, which decrease and become zero when local coverage of a monolayer is achieved. Short-range lateral interaction affects only nearest neighboring molecules, at high surface coverage values ($\theta \approx 1$), as if the spacing between sites is small. Long-range lateral interaction affects carbon monoxide molecules, also at high surface coverage but at lower value ($\theta < 1$). Then, while the larger amount of CO molecules is adsorbed on lower energy sites, at bigger distance from the surface, their adsorption is accompanied with attractive forces (B sites). The adsorption of CO into the pores is accompanied with much higher attractive interactions (sites C). Both B and mainly C active sites are indicative of the formation of CO islands.

The surface of the studied catalysts is characterized by an *intermediate* surface topography. According to the observations related to the synergism between Pt and Rh [12–14] the bimetallic catalyst should be characterized by a more "*random*" topography, increasing the probability of finding surface CO and oxygen in the vicinity of each other and leading to a higher catalytic activity. On the other hand, group

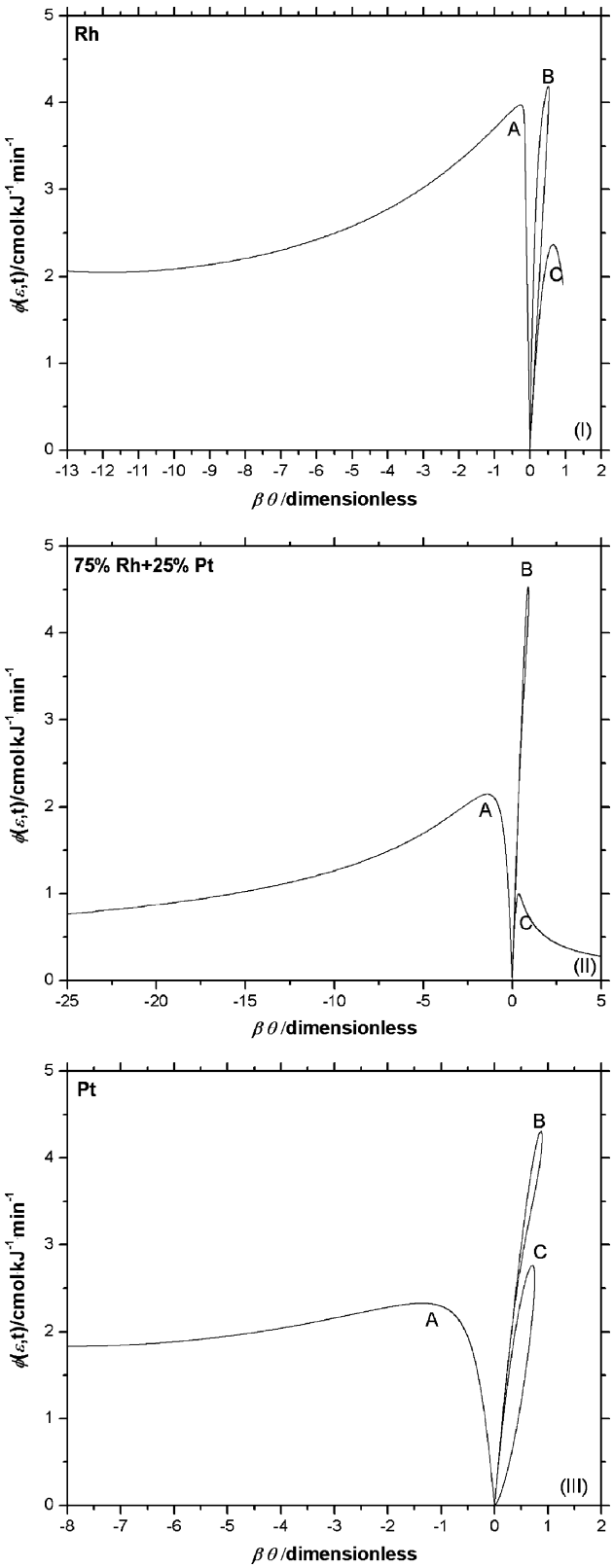

Fig. 8. Variation of the energy distribution function $\varphi(\varepsilon; t)$ against the product of the lateral interaction energy and the local isotherm, $\beta\theta$, for carbon monoxide adsorption over the following silica supported catalysts: (I) Rh_{pure}, at 445 °C, (II) $Pt_{0.25}$–$Rh_{0.75}$, at 390 °C, and (III) Pt_{pure}, at 425 °C. A, B and C indicate the three different groups of active sites corresponding to repulsive (A) and attractive (B and C) lateral interactions.

C active sites, corresponding to higher values of lateral interaction energy, are more characteristic of a "*patchwise*" topography.

Finally, the different groups of active sites, estimated by means of RF-GC are compared with thermal desorption spectroscopy (TDS) measurements. TDS yields in a simple way information about the number of binding states and their bond strengths with the surface. TDS of CO on group VIII metal surfaces in general show various peaks, which are classified into three main groups as shown schematically in Fig. 4 of Ref. [10]:

(1) Low-temperature γ states desorbing at temperatures much lower than room temperature.
(2) α States with a peak maximum in its TDS between 350 and 500 K.
(3) Sometimes depending on the metal, its surface structure and the experimental conditions (such as the temperature), additional states (β) are observed with a maximum of approximately 900 K. These β states arise from CO dissociation followed by recombination of C and O at the desorption temperature.

Depending on the surface structure and CO coverage two or three α peaks are usually shown. The B and C groups of active sites shown in our plots, correspond to energies in which α states are shown in TDS. They are rationalized on the basis of distinct species adsorbed on different sites and in terms of lateral interactions. They correspond to the molecular adsorption of carbon monoxide. At higher coverages, the overlayer unit cell is compressed, new surface structures are observed and a fraction of CO molecules are forced to move into their sites. At the highest coverage, a close-packed overlayer is formed, which is largely determined by CO–CO mutual repulsion and not by substrate sites. In this case CO may acts as a bridging ligand [10].

β States, arising from CO dissociation are expected to be observed at higher energies and temperatures, where dissociation prevails. Active sites of group A of our plots seem to correspond very well to the β states of TDS. This is clearly shown in the plots of the distribution function against the adsorbed concentration of CO, shown in Fig. 6. The probability of group A active sites, which correspond to higher adsorption energies, increase with increasing temperature.

Oscillatory behavior has been reported for CO oxidation on group VIII metal surfaces. However, under the experimental conditions of our studies ($T > 610$ K and $P = 1.33$ atm) oscillatory behavior has not been reported and does not affect our results [32].

5. Conclusions

(i) An inverse gas chromatographic instrumentation, this of reversed-flow gas chromatography, was used for the study of adsorption on heterogeneous surfaces. The presented methodology is technically very simple and it is combined with a mathematical analysis that gives the possibility for the estimation of various physicochemical parameters related with the adsorption on heterogeneous surfaces in a simple experiment under conditions compatible with the operation of real catalysts. The found, by means of RF-GC, energy distribution functions suggest the existence of three groups of active sites.

(ii) Group A active sites correspond to high values of coverage and adsorption energy, indicating the chemisorption of CO on the minima of potential energy of the surface. The mobility of carbon monoxide on group A active sites is limited, as concluded by the found D_s values. The topography of these active sites is random, as the values of the lateral interaction energy, β, are negative. Group A active sites correspond to β states of TDS, arising from CO dissociative adsorption.

(iii) Groups B and C of active sites, by means of RF-GC, correspond to the molecular adsorption of CO at sites of lower energy and surface coverage. They are characterized by positive values of β, which means that they have a patchwise topography. New adsorption sites are created by lateral interactions with already adsorbed molecules and a fraction of CO molecules may bound to chemisorbed CO molecules (part B). Group C active sites correspond to higher β values, in comparison with B group active sites. They are indicative of CO island formation. The bonding of CO on these sites is less strong and the mobility of CO molecules is much higher. Group C active sites should be associated with a reconstruction of the surface. The B and C groups of active sites shown in our plots, probably correspond to α states of TDS.

(iv) The experimentally found results explain the superior activity of $Pt_{0.25} + Rh_{0.75}$ alloy catalyst as result not only of its capacity to adsorb higher amount of carbon monoxide, at lower temperatures, but also due to the fact that this catalyst is characterized by a more random topography in contrast with the other studied pure Pt and Rh catalysts. These results are also consistent with those presented by other researchers, for the same catalysts, using different techniques.

References

[1] W. Rudzinski, D.H. Everett, Adsorption of Gases on Heterogeneous surfaces, Academic Press, London, 1992.
[2] W. Rudzinski, W.A. Steele, G. Zgrablich. Equilibria and Dynamics of Gas Adsorption on Heterogeneous Solid Surfaces, Elsevier Amsterdam, 1997.
[3] A.W. Adamson, Colloids Surf. A 118 (1996) 193.
[4] H. Balard, Langmuir 13 (1997) 1260.
[5] D.J. Williams (Guest Editor), J. Chromatogr. A 969 (2002) 3.
[6] N.A. Katsanos, E. Iliopoulou, F. Roubani-Kalantzopoulou, E. Kalogirou, J. Phys. Chem. B 103 (1999) 10228.
[7] N.A. Katsanos, D. Gavril, G. Karaiskakis, J. Chromatogr. A 983 (2003) 177.

[8] N.A. Katsanos, F. Roubani-Kalantzopoulou, E. Iliopoulou, I. Bassiotis, V. Siokos, M.N. Vrahatis, V.P. Plagianakos, Colloids Surf. A 201 (2002) 173.
[9] S.H. Oh, S. Sinkevitch, J. Catal. 142 (1993) 254.
[10] B.E. Nieuwenhuys, Adv. Catal. 44 (1999) 259.
[11] N.A. Katsanos, G. Karaiskakis, Adv. Chromatogr. 24 (1984) 125.
[12] R.M. Wolf, J. Siera, F.C.M.J.M. van Delft, B.E. Nieuwenhuys, Faraday Discuss. Chem. Soc. 87 (1989) 275.
[13] F.C.M.J.M. van Delft, B.E. Nieuwenhuys, J. Siera, R.M. Wolf, ISIJ Int. 29 (1989) 550.
[14] S.H. Oh, J.E. Carpenter, J. Catal. 98 (1986) 178.
[15] D. Gavril, N.A. Katsanos, G. Karaiskakis, J. Chromatogr. A 852 (1999) 507.
[16] D. Gavril, A. Koliadima, G. Karaiskakis, Langmuir 15 (1999) 3798.
[17] D. Gavril, A. Koliadima, G. Karaiskakis, Chromatographia 49 (1999) 285.
[18] D. Gavril, J. Liq. Chromatogr. Rel. Technol. 25 (2002) 2079.
[19] D. Gavril, Instrum. Sci. Technol. 30 (2002) 397.
[20] D. Gavril, V. Loukopoulos, G. Karaiskakis, Chromatographia 59 (2004), in press.
[21] A.J. Ramirez-Pastor, D. Stacchiola, M.S. Nazzarro, J. L Riccardo, G. Zgrablich, Surf. Sci. 449 (2000) 43.
[22] W.A. Steele, Appl. Surf. Sci. 7820 (2002) 1.
[23] J. Jagiello, Langmuir 10 (1994) 2778.
[24] N.A. Katsanos, E. Iliopoulou, V. Plagianakos, H. Mangou, J. Colloid Int. Sci. 239 (2001) 10.
[25] P. Schneider, J.M. Smith, AIChE J. 14 (1968) 762.
[26] Y. Yashuda, J. Phys. Chem. 86 (1982) 1913.
[27] P.L.J. Mayfield, D.D. Do, Ind. Eng. Chem. Res. 30 (1991) 1262.
[28] Y.D. Chen, R.T. Yang, Carbon 36 (1998) 1525.
[29] E.N. Fuller, P.D. Schettler, J.C. Giddings, Ind. Eng. Chem. 58 (1966) 19.
[30] B. Hellsing, V.P. Zhdanov, Chem. Phys. Lett. 147 (1988) 613.
[31] R. Fowler, E.A. Guggenheim, Statistical Thermodynamics, Cambridge University Press, Cambridge, 1952.
[32] T. Ioannides, A.M. Efstathiou, Z.L. Zhang, X.E. Verykios, J. Catal. 156 (1995) 265.